A&A 372, L13–L16 (2001)
DOI: 10.1051/0004-6361:20010540

Astronomy & Astrophysics

Radiative properties of magnetic elements

I. Why are G-band bright points bright?

O. Steiner[1], P. H. Hauschildt[2], and J. Bruls[1]

[1] Kiepenheuer-Institut für Sonnenphysik, Schöneckstrasse 6, 79104 Freiburg, Germany
[2] The University of Georgia, Dept. of Physics & Astronomy, Athens, GA 30602-2451, Greece

Received 1 February 2001 / Accepted 11 April 2001

Abstract. Photospheric magnetic elements are most conspicuously visible in high-resolution G-band filtergrams. We show that their enhanced contrast in the G-band is due to a reduction of the CH abundance by dissociation in the deep photospheric layers of the flux tube, where it is hotter than in the surrounding atmosphere. As a consequence, the CH-lines weaken, allowing more of the continuum to "shine" through the forest of G-band CH-lines. We suggest that other molecular bands or atomic lines may exhibit a similar behaviour.

Key words. Sun: photosphere – Sun: magnetic fields – Sun: faculae, plages – solar irradiance variability – G-band

1. Introduction

G-band filtergrams of the solar surface obtained since 1984 by various groups (Muller & Roudier 1984; Brandt et al. 1994; Berger et al. 1995; Löfdahl et al. 1998; Sigwarth et al. 2000; Sütterlin 2001) have much attracted the attention of solar physicists. If obtained at a high enough spatial resolution, these images show brilliant bright points that are a manifestation of small scale magnetic flux concentrations in the photosphere, so-called magnetic elements. Recently, Langhans et al. (2001) have recorded a section the G-band spectrum of isolated G-band bright points.

The physical reason for magnetic elements having exceedingly high contrast in the G-band has remained enigmatic, although various explanations were offered by Rutten (1999). Sánchez Almeida et al. (2001) and Rutten et al. (2001) come in studies carried out independently from the present one to similar conclusion as offered here.

The enhanced brightness of plage and network magnetic elements, is thought to be an important component of solar irradiance variability, as their coverage fraction over the solar disk changes with solar cycle (Lean & Foukal 1988; Fligge et al. 2000). The radiative properties of magnetic elements, or their proxy counterpart, the "G-band bright points", are therefore of great interest.

In this paper, we present results from synthetic G-band spectra computed on the basis of empirical, plane-parallel model atmospheres and show why the contrast of bright points is so much higher in the G-band than it is in the continuum. We adopt the LTE assumption, leaving an estimate of the deviation from LTE and the effect of the geometrical structure of magnetic elements to a forthcoming paper in this series.

Send offprint requests to: O. Steiner,
e-mail: steiner@kis.uni-freiburg.de

2. Model atmospheres

G-band bright points are a manifestation of magnetic elements, which are concentrations of magnetic flux into tube-like structures in the photosphere. In this study, however, the geometrical structure of magnetic flux tubes is discarded but instead, their atmosphere considered to be plane-parallel. This implies, that we do not attempt to mimic finite spatial resolution of G-band bright-point observations or any filling factor. Instead, synthetic results will be compared with contrast measurements that are corrected for the limited spatial resolution by means of instrumental and atmospheric modulation transfer functions, i.e., with intrinsic contrast values. Thus, only the substructure of the magnetic element atmosphere (e.g., hot walls) will be neglected in the computation of synthetic G-band spectra. We think that this simplification is admissible, reminding that the empirical atmospheres too, are actually an average over such substructure. To take them properly into account would require a NLTE-calculation.

Here we use the empirically derived model atmospheres for network (`net`) and plage (`pla`) flux tubes of Solanki & Brigljević (1992) for models of the flux tube atmosphere and compare the resulting spectra with that of the surrounding quiet Sun reference atmosphere (`FWFAK_C`) of Fontenla et al. (1999), which applies to the average

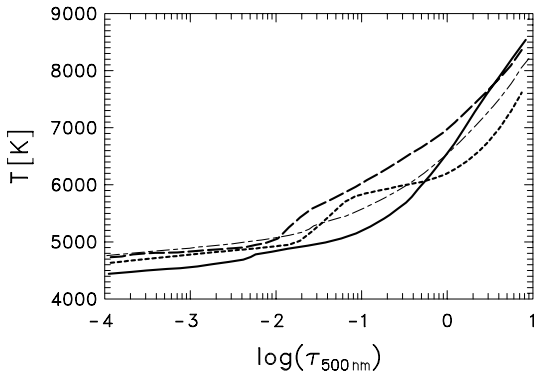

Fig. 1. Temperature as a function of continuum optical depth $\tau_{500\,\mathrm{nm}}$ of the modified quiet Sun model `FWFAK_C` (——) and the bright plage model `FWFAK_P` (–·–·–) of Fontenla et al. (1999), together with the magnetic flux tube atmospheres `net` (network elements, – – –) and `pla` (plage elements, ·····) of Solanki & Brigljević (1992).

supergranule cell interior. The latter is modified in that the chromospheric temperature increase is replaced by a linear extrapolation of the photospheric temperature decrease of 1 K/km. With this modification we avoid spurious line core emission reversals of strong absorption lines as a consequence of the LTE treatment. The models of Solanki & Brigljević should be particularly good in the deep photospheric layers to which the following analysis applies. They are derived from Stokes spectra of polarized light (similar to the models of Keller et al. 1990) and therefore apply to the magnetic flux concentration proper, different from more conventional models of bright structures such as `FWFAK_P`, which we also use in this analysis. Figure 1 shows the temperature as function of optical depth for the various models.

3. Synthetic *G*-band spectrum and contrast

We use the radiation transfer code PHOENIX (Hauschildt et al. 1996; Hauschildt et al. 1997, 1999) in order to compute synthetic *G*-band spectra and continuum radiation from each model atmosphere, assuming all models to be plane-parallel. This code includes a master line list of 47 million atomic and up to 350 million molecular lines. The molecular line list includes the HITRAN92 list (Rothman et al. 1992) as well as Kurucz's CD 15 data (Kurucz 1993). Additional lists complete or replace HITRAN92 or CD 15, whenever they are judged more reliable. Line profiles are assumed to be depth-dependent Voigt profiles, or Doppler profiles for very weak lines only. Details of the computation of the damping constants and the line profiles are given in Schweitzer et al. (1996). For all calculations we use a height-independent microturbulence of 1 $\mathrm{km\,s^{-1}}$.

Figure 2a shows the synthetic *G*-band intensity spectrum from 429.6 nm to 431.8 nm computed from the quiet Sun model `FWFAK_C` (thick curve) together with the corresponding observed spectrum as given in the "Jungfraujoch atlas" (Delbouille et al. 1989), both for disk center. Note

Table 1. Contrast of three model atmospheres against the quiet Sun reference `FWFAK_C` from synthetic reconstruction of the *G*-band, the continuum, and the "*G*-band" void of CH-lines.

	net	pla	`FWFAK_P`
C_G	1.34	0.28	0.39
C_c	0.33	−0.22	−0.03
$C_{G'}$	0.66	−0.05	0.12

that vacuum wavelengths are given. The agreement between the two spectra is impressive: almost all the observed lines and blends are correctly reproduced and the rms deviation over the full wavelength range is 0.11. The indicated line identification is from the computation, given for the strongest line at each wavelength position if above a certain threshold.

Figure 2b shows the synthetic *G*-band spectrum of the network model, `net` (thin curve), together with that of the quiet Sun model, `FWFAK_C` (thick curve) and with the continuum intensity attenuated by the transmission profile of the *G*-band pass filter (dashed curve). The `net`-model shows a higher intensity throughout because it is hotter than the quiet Sun model, but the difference is more pronounced within ranges of CH-band lines than in the continuum and many other spectral lines. This can be quantified by comparing the contrast in the continuum, C_c, with that over the entire bandpass filter of the two spectra, C_G:

$$C_\mathrm{c} = \frac{(I_{\mathrm{bp\,c}} - I_{0\,\mathrm{c}})}{I_{0\,\mathrm{c}}}, \quad \text{and} \quad C_G = \frac{\int T_G (I_\mathrm{bp} - I_0)\,\mathrm{d}\lambda}{\int T_G I_0\,\mathrm{d}\lambda}.$$

Here, index c refers to the theoretical continuum at 430 nm, index bp to the flux tube atmosphere (bright point), and index 0 to the quiet Sun model atmosphere. I designates the intensity and T_G is the *G*-band transmission profile. The integration is taken from 428.4 to 432.6 nm. Additionally, we also compute the "*G*-band" contrast from the synthetic spectra where the molecule CH was discarded in the radiation transfer, calling it $C_{G'}$.

Table 1 compiles all the computed contrast values for which always the same quiet Sun reference-atmosphere, `FWFAK_C`, was used. For the network model atmosphere the contrast in the *G*-band is a factor of 4.06 higher than the corresponding value in the continuum. This enhancement factor is considerably higher than the factor of two reported by Berger et al. (1995) but the quantity is not well defined as demonstrated by (Steiner et al. 2001). Also the *G*-band contrast of 1.34 is much higher than the maximum *intrinsic* contrast of 0.5 found by Title & Berger (1996) of network elements. In this paper, however, we endeavor to understand the cause of the contrast enhancement rather than to reproduce precise contrast values.

4. What causes the enhanced *G*-band contrast?

Figure 3 shows the partial gas pressure (which is directly proportional to the (ionic) abundance) of CH, CO, CN, Fe I, Fe II, and Ti II as a function of optical depth $\tau_{500\,\mathrm{nm}}$ for

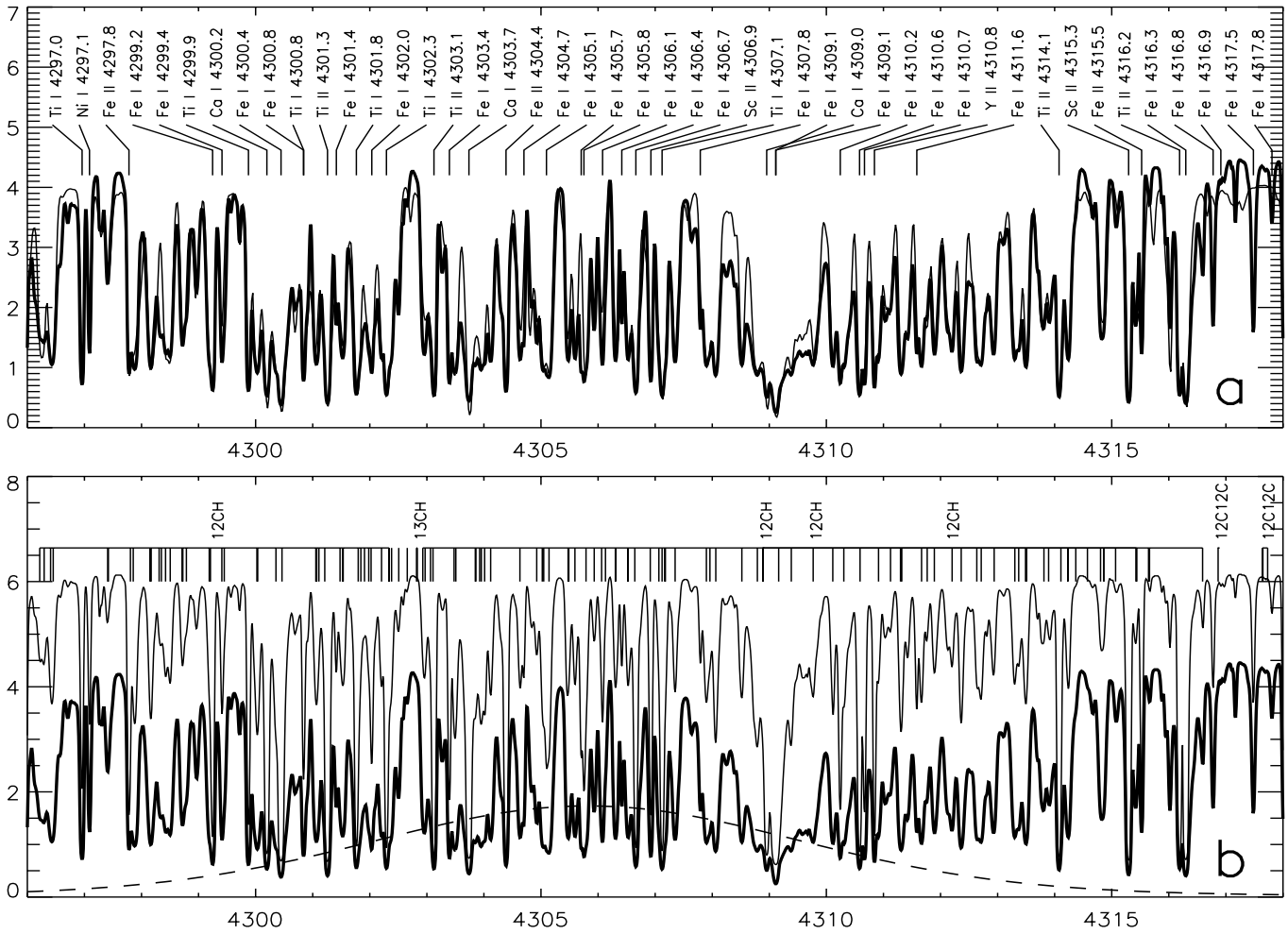

Fig. 2. a) Synthetic G-band spectrum (thick line curve) from 429.6 nm to 431.8 nm computed on the basis of the quiet Sun model `FWFAK_C` (Fontenla et al. 1999). Wavelengths correspond to vacuum wavelengths in Å, the intensity is given in $\mathrm{W\,cm^{-2}\,ster^{-1}\,nm^{-1}}$. The thin curve shows for comparison the observed spectrum from the "Jungfraujoch" atlas (Delbouille et al. 1989). Atomic line identifications are from the computation. **b)** Synthetic G-band spectrum of the quiet Sun model `FWFAK_C` (thick line curve) together with the synthetic spectrum of the network flux-tube atmosphere `net` (Solanki & Brigljević 1992) (thin curve) and with the continuum intensity attenuated with the transmission profile of the G-band pass filter (dashed curve). Also indicated are molecular line positions.

the quiet Sun model `FWFAK_C` (thick curves) and the network model atmosphere `net` (thin curves). We first note that the relative pressure of CO increases much steeper with height than it does for CH, which eventuates from CO curtailing the formation of CH with increasing height, restricting its presence mainly to the deep photosphere (Rutten 1999). Accordingly, the line-core formation height of CH-lines in the G-band as computed with PHOENIX is at around 140 km, corresponding to $\tau_{500\,\mathrm{nm}} = 0.1$ in the quiet Sun model, which explains why G-band filtergrams and white light images of solar granulation look much alike.

In the network atmosphere, the CH relative pressure is markedly reduced with respect to the reference atmosphere in the optical depth range from $\tau_{500\,\mathrm{nm}} = 0.01$ to $\tau_{500\,\mathrm{nm}} \approx 3.0$, which includes the formation height for the CH lines of the G-band. This reduction is clearly because of `net` being up to 800 K hotter in this range causing CH with its low ionization potential of 3.5 eV, to dissociate. The shortfall of CH weakens the CH lines in the G-band of network bright points, allowing more of the continuum to "shine through the thinned forest" of CH-lines. From this, we conclude that the strong contrast enhancement of network bright-points in the G-band is due to the depletion of CH, induced by the temperature elevation in the deep layers of the network atmosphere with respect to the surrounding quiet Sun at equal optical depth. This effect must be separated from the direct influence of a temperature elevation on the line source function, which also brightens spectral lines but works without any change in the abundance of species. This latter effect is less important for the G-band contrast enhancement as can be seen from the extremely small difference between the two atmospheres in the cores of Fe II and Ti II lines, for which ions the partial pressures does not change (Fig. 3).

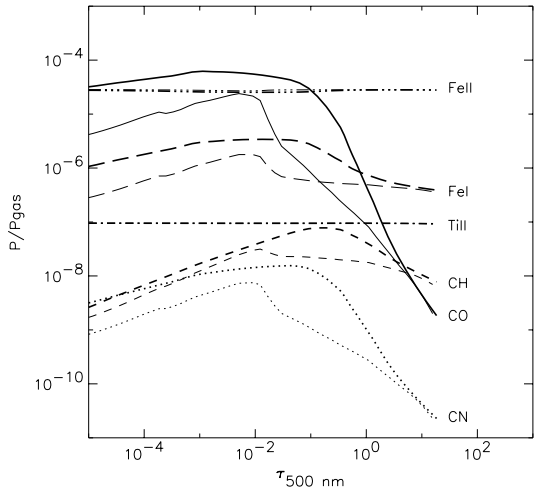

Fig. 3. Partial gas pressure as a fraction of the total gas pressure for the molecules CO, CH, and CN as a function of optical depth. Thick curves refer to the quiet Sun model, `FWFAK_C`, thin curves to the network element atmosphere, `net`. Also shown are the partial pressures of Fe I, Fe II, and Ti II, the ions being practically identical and constant for both atmospheres.

Although most, not all of the G-band contrast enhancement is accounted for by CH as can be seen from the difference between $C_{G'}$ and C_c (see Table 1). Figure 3 shows that Fe I behaves similarly to CH so that the multitude of Fe I lines within the G-band must prominently contribute to this difference. A close inspection of Fig. 2b verifies, that weak Fe I lines (that form in deep layers) are liable to a similar line weakening as lines of CH. This effect is likely present in most white light contrast measurements, since they always include many spectral lines of metallic neutrals. Therefore, the difference $C_G - C_{G'}$ is probably a more realistic value for the contrast enhancement relative to an impure continuum. A behaviour similar to CH is also exhibited by CN, so that we expect contrast enhancements similar to the G-band for example in the CN bandhead at 388.3 nm (see Chapman 1970). CO shows an even stronger difference between the two atmospheres for $\tau_{500\,nm} > 0.01$.

5. Conclusions

Computing synthetic G-band spectra from model atmospheres of the quiet Sun and network and plage magnetic flux tubes, we have shown that the enhanced contrast in the G-band is largely a consequence of enhanced CH depletion through molecular dissociation in the deep photospheric layers of the hotter flux-tube atmospheres compared to the quiet Sun surroundings. This process weakens the CH-lines within the flux tube, allowing more of the continuum to "shine through the thinned forest of CH-lines" across the G-band. Other molecular bandheads and many (weak) Fe I and other neutral metal lines across the spectrum are expected to expose a similar behaviour as CH.

We cannot falsify the conjecture of Rutten (1999) that photodissociation by UV-radiation from the hot walls may be an important mechanism of G-band contrast enhancement, since the present computation is in pure LTE. However, taken the present model atmospheres at face value, dissociation processes in LTE more than suffice to produce the observed contrast enhancement and additional photodissociation would further increase it.

Acknowledgements. We would like to thank S. K. Solanki and P. Fox for providing the atmosphere models.

References

Berger, T. E., Schrijver, C. J., Shine, R. A., et al. 1995, ApJ, 454, 531
Brandt, P. N., Rutten, R. J., Shine, R. A., & Trujillo Bueno, J. 1994, in Solar Surface Magnetism, ed. R. Rutten, & C. Schrijver, 251
Chapman, G. A. 1970, SP, 13, 78
Delbouille, L., Roland, G., & Neven, L. 1989, Photometrique Atlas of the Solar Spectrum (Univ. de Liège)
Fligge, M., Solanki, S. K., & Unruh, Y. C. 2000, A&A, 353, 380
Fontenla, J., White, O. R., Fox, P. A., Avrett, E. H., & Kurucz, R. L. 1999, ApJ, 518, 480
Hauschildt, P. H., Baron, E., Starrfield, S., & Allard, F. 1996, ApJ, 462, 386
Hauschildt, P. H., Allard, F., & Baron, E. 1999, ApJ, 512, 377
Hauschildt, P. H., Baron, E., & Allard, F. 1997, ApJ, 483, 390
Keller, C. U., Steiner, O., Stenflo, J. O., & Solanki, S. K. 1990, A&A, 233, 583
Kurucz, R. 1993, Molecular Data for Opacity Calculations, Kurucz CD-ROM, No. 15
Langhans, K., Rimmele, T., Sigwarth, M., & Schmidt, W. 2001, in Advanced Solar Polarimetry, ed. M. Sigwarth, ASP Conf. Ser., in press
Lean, J., & Foukal, P. 1988, Science, 240, 906
Löfdahl, M. G., Berger, T. E., Shine, R. S., & Title, A. M. 1998, ApJ, 495, 965
Muller, R., & Roudier, T. 1984, SP, 94, 33
Rothman, L. S., Gamache, R. R., Tipping, R. H., et al. 1992, J.Q.S.R.T, 48, 469
Rutten, R., Kiselman, D., Rouppe van der Voort, L., & Plez, B. 2001, in Advanced Solar Polarimetry, ed. M. Sigwarth, ASP Conf. Ser., in press
Rutten, R. J. 1999, in ASP Conf. Ser., 184, Magnetic Fields and Oscillations, ed. B. Schmieder, A. Hoffmann, & J. Staude, 181
Sánchez Almeida, J., Asensio Ramos, A., Trujillo Bueno, J., & Cernicharo, J. 2001, ApJ, in press
Schweitzer, A., Hauschildt, P. H., Allard, F., & Basri, G. 1996, MNRAS, 283, 821
Sigwarth, M., Rimmele, T., Richards, K., et al. 2000, NOAO Newsletter, 63, 5
Solanki, S. K., & Brigljević, V. 1992, A&A, 262, L29
Steiner, O., Bruls, J., & Hauschildt, P. 2001, in Advanced Solar Polarimetry, ed. M. Sigwarth, in press
Sütterlin, P. 2001, in Advanced Solar Polarimetry, ed. M. Sigwarth, ASP Conf. Ser., in press
Title, A. M., & Berger, T. E. 1996, ApJ, 463, 797